NATIONAL ADVISORY COMMITTEE FOR AERONAUTICS

TECHNICAL NOTE 2029

THE INTERPRETATION OF BIAXIAL-TENSION EXPERIMENTS INVOLVING CONSTANT STRESS RATIOS

By S. B. Batdorf

Langley Aeronautical Laboratory
Langley Air Force Base, Va.

Washington
February 1950

NATIONAL ADVISORY COMMITTEE FOR AERONAUTICS

TECHNICAL NOTE 2029

THE INTERPRETATION OF BIAXIAL-TENSION EXPERIMENTS INVOLVING CONSTANT STRESS RATIOS

By S. B. Batdorf

SUMMARY

The slip theory of plasticity is applied to the problem of calculating the strains associated with biaxial tension for the case of constant stress ratios and is found to be in better agreement with experiment than the octahedral-shear and maximum-shear theories usually employed to analyze such data.

INTRODUCTION

The mathematical theory of plasticity is concerned with solving over a wider stress range much the same sort of problem as that treated in the elastic range by the theory of elasticity. To solve such problems the stress-strain relations for the material must be known. This requirement presents no particular obstacle in the solution of problems in which only a single type of stress occurs, for the stress-strain relations for tension, compression, and shear are known or can be established by standardized tests. However, the stress-strain relations corresponding to combined stresses have not yet been definitely established.

Among the wide variety of possible types of loading involving combined stresses, the simplest case, from a theoretical point of view, is that in which the stress ratios and directions are kept constant. Also, this case corresponds approximately to the loading conditions encountered in a number of structural applications.

The behavior of metals subjected to a two-dimensional state of stress in which the ratio and direction of the principal stresses are held constant has been the subject of a large number of experimental investigations. (For a few examples, see the bibliography at the end of this paper.) The results have usually been interpreted in terms of a generalized stress-strain curve in which a function of the applied stresses is plotted against a function of the resulting strains. These functions, which are sometimes called the stress intensity and

strain intensity, or the effective stress and effective strain, reduce simply to the applied stress and the corresponding strain or a multiple of them when only a single type of stress is present.

Recently a theory for the polyaxial stress relations in the plastic range was advanced which takes explicit account of the polycrystalline nature of metals (reference 1). In this approach, which is based on the assumption that plastic deformation is due to slip within the individual grains, concepts such as stress intensity and strain intensity play no part.

The present paper is concerned with the interpretation of biaxial-tension experiments involving constant directions and ratios of the stresses, from the point of view of the slip theory. A comparison is made with the experimental results of W. R. Osgood (reference 2). This experimental investigation was selected because it includes data in the regions of small strain to which the slip theory in its present form is thought to be applicable (reference 3), because the material employed exhibited strain hardening and appears to have been reasonably isotropic initially, as assumed in the theory, and because the investigation shows evidence of having been very carefully carried out. The cooperation of Dr. Osgood and the National Bureau of Standards in supplying the original data obtained in the investigation is gratefully acknowledged.

SYMBOLS

Ω	solid angle, used to describe orientation of slip planes, steradians
β	angular coordinate giving direction of slip, radians
σ	normal stress
σ_L	normal stress at which plastic deformation begins
σ_I, σ_{II}, σ_{III}	principal stresses, $\sigma_I > \sigma_{II} > \sigma_{III}$
τ	shear stress
τ_L	shear stress at which plastic deformation begins
ϵ	total normal strain

ϵ''	plastic strain
ϵ_I'', ϵ_{II}'', ϵ_{III}''	principal plastic strains, corresponding in direction to σ_I, σ_{II}, and σ_{III}, respectively
γ	total shear strain
γ''	plastic shear strain
x,y,z	coordinates taken in the axial, circumferential, and radial directions of the cylinder, respectively, and also used as subscripts in connection with stress and strain to denote particular components of these quantities
1,2	direction of normal to slip plane and direction of slip, respectively
F, $F(\tau_{12})$	characteristic shear function for material, giving plastic shear strain per steradian of slip-plane orientation per radian of slip direction as a function of shear stress
l_{x1}, l_{y1}, . . . l_{z2}	cosines of angles between x and 1, y and 1, . . . z and 2 directions
a_n	coefficient of nth term in series expansion for F
g_n, $g_n\left(\frac{\sigma}{\sigma_L}\right)$	function giving variation of plastic strain with applied stress in uniaxial compression or tension, corresponding to nth term of series expansion for F
θ	angle between slip-plane normal and polar direction in polar coordinate system
E	Young's modulus for the material
E_s	secant modulus for the material

FUNDAMENTALS OF THE SLIP THEORY

According to the slip theory of plasticity (reference 1), plastic action is caused by slip in unfavorably oriented grains. The strain

associated with a given state of stress is determined by finding the plastic shear strain associated with slip in a given plane and a given direction, resolving this plastic shear strain into plastic strains in a convenient fixed set of coordinates, and summing over all slip planes and slip directions. The plastic shear strain associated with planes whose normals are included in the solid angle $d\Omega$ about direction 1 (see fig. 1) and with slip directions included in the angle $d\beta$ about direction 2 is given by

$$d\gamma_{12}'' = F(\tau_{12})d\Omega\, d\beta \tag{1}$$

where F is a function depending only on the history of τ_{12}, the shear stress in the 2-direction which is acting on the plane perpendicular to the 1-axis. If the stress history is such that reverse slip does not occur, F depends only on the highest previous value of the shear-stress component in question, which is the instantaneous value of the shear-stress component in the case of constant stress ratio and continual loading.

The infinitesimal shear strain is resolved into strains in the standard x, y, and z axes by means of the strain-transformation equations of the theory of elasticity, which may be written in the form

$$\left.\begin{aligned} d\epsilon_x'' &= l_{x1}l_{x2}\, d\gamma_{12}'' \\ &\cdots\cdots \\ d\gamma_{xy}'' &= \left(l_{x1}l_{y2} + l_{y1}l_{x2}\right)d\gamma_{12}'' \\ &\cdots\cdots \end{aligned}\right\} \tag{2}$$

The total plastic strains in the standard axes thus become

$$\left.\begin{aligned} \epsilon_x'' &= \int\int l_{x1} l_{x2} F\left(\tau_{12}\right) d\Omega \, d\beta \\ \gamma_{xy}'' &= \int\int \left(l_{x1} l_{y2} + l_{x2} l_{y1}\right) F\left(\tau_{12}\right) d\Omega \, d\beta \end{aligned}\right\} \tag{3}$$

in which the integration with respect to Ω extends over a hemisphere and that with respect to β extends over 180°.

If the applied stresses are given in the standard coordinate system as σ_x, σ_y, . . . τ_{yz}, the shear stress is given by

$$\begin{aligned} \tau_{12} = {} & l_{x1} l_{x2} \sigma_x + l_{y1} l_{y2} \sigma_y + l_{z1} l_{z2} \sigma_z + \left(l_{x1} l_{y2} + l_{y1} l_{x2}\right) \tau_{xy} \\ & + \left(l_{x1} l_{z2} + l_{z1} l_{x2}\right) \tau_{xz} + \left(l_{y1} l_{z2} + l_{z1} l_{y2}\right) \tau_{yz} \end{aligned} \tag{4}$$

The total plastic strains can be determined from equations (3) and (4) when the characteristic shear function F is known. This function can be found from the tensile or compressive stress-strain curve (assumed in the theory to be identical) by the use of the following equation:

$$F\left(\tau_{12}\right) = \sum_{n=1}^{N} a_n \left(\frac{\tau_{12}}{\tau_L} - 1\right)^n \tag{5}$$

for $\tau_{12} \geq \tau_L$.

The coefficients a_n in equation (5) are determined by writing the equation

$$\epsilon'' = \sum_{n=1}^{N} a_n g_n \left(\frac{\sigma}{\sigma_L}\right) \tag{6}$$

for a set of N different stress levels and solving them simultaneously. In this equation, σ_L is the elastic limit as ascertained from the stress–strain curve, ϵ'' is the plastic strain corresponding to the stress level σ, and the quantities g_n are given in table 1 for five stress levels above the elastic limit for the material.

EXPERIMENTAL DATA AND PREVIOUS ANALYSES

In Osgood's investigation (reference 2), biaxial–tension tests were made on five 24S–T aluminum–alloy tubes of $1\frac{3}{4}$–inch internal diameter, and 0.05–inch thickness. The nominal ratios of circumferential to axial stress were 0, 0.5, 1, 2, and ∞. The results were presented in the form of two generalized stress–strain curves for each ratio of stresses, namely, maximum shearing stress plotted against maximum shearing strain and octahedral shearing stress plotted against octahedral shearing strain. It was found that in each type of plot the data for stress ratios 0, 1, and ∞ fell for practical purposes along one curve, whereas the data for stress ratios 0.5 and 2 fell along another. In the plot of maximum shearing stress against maximum shearing strain, the curve for stress ratios 0.5 and 2 fell above the curve for stress ratios 0, 1, and ∞, whereas in the plot for octahedral shearing stress against octahedral shearing strain the reverse was true.

The fact that the generalized stress–strain curves for stress ratios 0 and ∞ coincide and that those for stress ratios 0.5 and 2 coincide is to be expected for an isotropic material. D. C. Drucker (reference 4) has pointed out that the coincidence of the curve for stress ratio 1 with those for stress ratios 0 and ∞ is also to be expected because the state of equal tension in the circumferential and axial directions differs from the state of compression in the thickness direction only by hydrostatic pressure, that is, a state of equal compression in the three principal directions. (Experiments have shown that plastic action is relatively insensitive to hydrostatic pressure.) He also showed that by a suitable choice of stress–intensity function a

result intermediate between the predictions of maximum-shear and octahedral-shear theories is obtained and the stress-strain curves for all five stress ratios can be brought into approximate coincidence.

QUALITATIVE CONSIDERATION OF BIAXIAL TENSION ON BASIS OF SLIP THEORY

The slip theory accounts for the data on the basis of entirely different considerations. According to this theory, when a material is tested in uniaxial tension, slip will first occur in those planes which make an angle of 45° with the direction of tension. For discussing plane orientations at a point, it is convenient to consider a sphere surrounding the point. Any plane through the point can then be represented by that radius of the sphere which is normal to it. The normals to the planes making an angle of 45° with the tensile direction intersect the sphere along a circular line (see fig. 2). As the tensile stress σ increases beyond the elastic limit σ_L, the line widens into a zone, the limiting circles of which are given by the first two roots of the equation

$$\theta = \frac{1}{2} \sin^{-1} \frac{\sigma_L}{\sigma} \tag{7}$$

The zones containing the normals of the slip planes for tension in the x- and y-directions, respectively, together with the corresponding directions of resolved shear stress are shown in figures 3(a) and 3(b). If the two stresses are equal and are applied simultaneously, as shown in figure 3(c), the resolved shear stress becomes zero in location A, but is equal to the value for σ_x alone at location B, and for σ_y alone at location C. The area containing the normals of the slip planes in this case turns out, in fact, to be a zone related to the z-axis in the same way the previously discussed zones were related to the x- and y-axes. If due account is taken of the direction of the shear stress, it becomes evident that the simultaneous tensions $\sigma_x = \sigma_y = \sigma$ are equivalent to the compression $\sigma_z = -\sigma$, a result also derivable by the addition of a hydrostatic pressure, as noted in the previous section. The three stress states illustrated in figure 3 correspond to the stress ratios 0, 1, and ∞. Inasmuch as the plastic deformation in a given plane is assumed to be determined solely by the shear stress in that plane, the slip theory predicts that with proper permutation of axes the relationship between applied stress and resulting strain is the same for all three stress states; as previously noted, this prediction was experimentally verified.

If tensions σ_x and σ_y are unequal, a different situation arises, which, for simplicity, is discussed in terms of the symbols for principal stress $\sigma_I > \sigma_{II} > \sigma_{III}$. Consider for example the case in which $\sigma_I = 2\sigma_{II}$, $\sigma_{III} = 0$. As the two stresses are increased in ratio, slip will first occur at the same value of σ_I as though σ_{II} were not present. However, instead of occurring in all the planes whose normals lie along the 45° circle, it will occur only in the planes whose normals pierce the circle at points B and B' (see fig. 4), and, instead of growing into a zone bounded by two parallel circles as in the case of increasing uniaxial tension, the area enclosing the slip-plane normals will become roughly a pair of ellipses, as indicated in the figure, which merge when $\sigma_I = 2\sigma_{II} = 2\sigma_L$. Figure 4 shows that, because of the presence of σ_{II}, fewer planes participate in the plastic deformation than would participate if σ_I alone were acting, so that the total plastic strain is decreased by the presence of σ_{II}. Thus, the slip theory predicts an elastic limit in agreement with that predicted by maximum-shear theory, but the strains corresponding to stresses above the elastic limit are determined not by the maximum value of the shear alone, but by the total state of stress. Figure 5 indicates that Osgood's data verify the reduction in strain due to the presence of the second stress but do not give an elastic limit depending only on the larger stress as the preceding discussion would lead one to expect.

A reason for this discrepancy is not difficult to find. Even aside from variations in material properties, verification of the prediction that the value of σ_I corresponding to the elastic limit for the material is the same whether $\sigma_{II} = 0$ or $\frac{1}{2}\sigma_I$ would be difficult by experimental means because plastic deformation must be of some finite magnitude to be experimentally evident. In rough approximation the elastic limit experimentally observed for $\sigma_{II} = 0$ and for $\sigma_{II} = \frac{1}{2}\sigma_I$ will correspond to equal areas of the regions on the sphere containing the normals to the slip planes in the two cases. Reference to figure 4 shows that the criterion of equal areas implies that the elastic limit observed for σ_I when $\sigma_{II} = \frac{1}{2}\sigma_I \left(\frac{\sigma_y}{\sigma_x} = 0.5 \text{ and } 2\right)$ will be above that observed when $\sigma_{II} = 0 \left(\frac{\sigma_y}{\sigma_x} = 0, 1, \text{ and } \infty\right)$. This result is verified on the average by the data in figure 5.

QUANTITATIVE TREATMENT OF BIAXIAL TENSION ON BASIS OF SLIP THEORY

The analysis of data in terms of the slip theory of plasticity requires a knowledge of the uniaxial stress–strain curve for the material (the material is assumed to be isotropic). Osgood's stress–strain data (reference 2) for the five stress ratios 0, 0.5, 1, 2, and ∞ fall into two groups. Stress ratios 0, 1, and ∞ correspond to uniaxial stress, and stress ratios 0.5 and 2 correspond to essentially the same state of combined stress. The analysis assumes the uniaxial stress–strain curve to be given and computes the plastic strains corresponding to stress ratio 0.5.

In figure 6, stress–strain data are given for stress ratios 0, 1, and ∞. For the cases of axial tension $\left(\frac{\sigma_y}{\sigma_x} = 0\right)$ and circumferential tension $\left(\frac{\sigma_y}{\sigma_x} = \infty\right)$ the stress is plotted against the corresponding strain. For the case $\left(\frac{\sigma_y}{\sigma_x} = 1\right)$ the equivalent radial stresses and corresponding radial strains were computed on the basis of the assumptions that volume does not change during plastic deformation and that hydrostatic pressure has no effect. The close correlation of the data corresponding to uniaxial stress in the three principal directions is evidence that the material used was probably very nearly isotropic.

The stress–strain data for the various stress ratios, however, are not equally reliable representations of the uniaxial properties of the material. The curves for stress ratios 1 and ∞ required the elimination of the axial stress by a proper balancing of internal pressure and axial compression on the tubular specimen, which elimination, as a practical matter, could only be made approximately; moreover, small experimental errors occurred because the state of circumferential stress was not entirely uniform over the thickness of the tube. The curve for stress ratio 0 was therefore chosen as the stress–strain curve for the material.

Before plastic strain can be computed, the characteristic shear function for the material must be determined. The determination of the characteristic shear function for the material required the solution of equation (6) for the coefficients a_n and the substitution of the results into equation (5). The elastic limit σ_L for the material was taken to be 36 ksi, and the plastic strains corresponding to the higher stress

levels for which the quantities g_n appearing in equation (6) have been computed (table 1) were taken to be those given in the following table:

$\frac{\sigma_I}{\sigma_L}$	ϵ''
1	0
1.10	.00015
1.25	.00085
1.40	.0046
1.60	.0200
1.80	.0530

The substitution of the values found for the coefficients a_n into equation (5) resulted in the characteristic shear curve given in figure 7.

The plastic shear strains corresponding to a given state of stress are determined by integrating over all orientations of slip planes and over all slip directions, as indicated in equations (3). The method employed for these integrations was the numerical one described in appendix C of reference 1. The following table gives the computed plastic strains for the case $\sigma_I = 2\sigma_{II}$, $\sigma_{III} = 0$:

$\frac{\sigma_I}{\sigma_L}$	ϵ_I''	ϵ_{II}''
1	0	0
1.2	.00012	0
1.4	.00133	0
1.6	.0070	0
1.8	.0193	0

The values for ϵ_{II}'' are known to be 0 because the state of stress is equivalent, except for hydrostatic pressure, to pure shear in the I, III - plane. The numerical computations did not, of course, give 0, but small negative numbers amounting in each case to less than 1 percent of the corresponding value for ϵ_I''; this result provides some indication of the order of accuracy of the numerical method employed.

COMPARISON WITH EXPERIMENT AND WITH OTHER THEORIES

For the sake of simplicity, the assumption is sometimes made in theories of plasticity that the material is incompressible in the elastic as well as in the plastic range. This assumption is rather inaccurate in the region starting with the elastic limit of the material and extending somewhat above the yield stress, which is the region to which the considerations of the present paper are limited and the region of principal interest in many structural applications. Comparisons will therefore be made with other theories only in the more accurate form in which the strain is divided into an elastic part and a plastic part, each of which is associated with the appropriate value of Poisson's ratio.

Since the theories differ only in regard to the plastic part of the strain, the usual mode of representation of results by means of plotting stress against total strain obscures the differences between the theories. Consider, for example, two stress–strain curves which correspond to a difference of a factor 2 in the plastic strain. Near the elastic limit the two curves are very close together because the plastic strain is only a small fraction of the total strain which is being plotted. At higher stresses, where the plastic strain is considerably larger than the elastic strain, the two curves are ordinarily still quite close together because in this region the slope is very small. Consequently, for a critical comparison of theories, a plot giving the relation between stress and plastic strain is preferable.

Such a plot is shown in figure 8. This figure compares the plastic strain ϵ_I'' as measured experimentally and as computed on the basis of slip theory, octahedral–shear theory, and maximum–shear theory. The experimental results were computed from test data of reference 2 by subtracting the elastic strains from the measured total strains on the basis of the assumptions that in the elastic range Young's modulus is 10.5×10^6 psi and Poisson's ratio is 0.305.

The results for octahedral–shear theory can be obtained by use of either Nadai's law or Laning's law (equations (30) and (33), respectively, of reference 5). For biaxial tension at constant stress ratio these laws can be shown to reduce to the following equations:

$$\epsilon_x'' = \left(\frac{1}{E_s} - \frac{1}{E}\right)\left(\sigma_x - \frac{1}{2}\sigma_y\right) \tag{8}$$

$$\epsilon_y'' = \left(\frac{1}{E_s} - \frac{1}{E}\right)\left(\sigma_y - \frac{1}{2}\sigma_x\right) \tag{9}$$

where the secant modulus E_s is taken as the slope of the line from the origin to the point on the stress–strain curve (fig. 6) corresponding to the stress level

$$\sigma = \sqrt{\sigma_x^2 + \sigma_y^2 - \sigma_x\sigma_y} \tag{10}$$

$$= \frac{\sqrt{3}}{2}\sigma_I \tag{11}$$

when

$$\sigma_I = 2\sigma_{II}$$

There does not appear to be a generally accepted and self-consistent maximum-shear theory for polyaxial stress–strain relations. However, the special case $\sigma_I = 2\sigma_{II} = 2\sigma$ turns out to be essentially equivalent to a state of pure shear, for the addition of a hydrostatic pressure equal to $-\sigma$ gives $\sigma_I = -\sigma_{III} = \sigma$, $\sigma_{II} = 0$. Thus in this special case maximum-shear theory makes a definite prediction of the biaxial stress–strain relations. From considerations of symmetry, $\epsilon_I'' = 0$. To find ϵ_{II}'', it is observed first of all that when the value of σ_I is given, τ_{max}, and therefore by maximum-shear theory γ_{max}'', is the same for simple tension and for the stress state under consideration. On the other hand, consideration of the Mohr strain circles involved shows that γ_{max}'' is $(3/2)\epsilon_I''$ and $2\epsilon_I''$, respectively, in the two stress states. Consequently, the presence of the stress $\sigma_{II} = \frac{1}{2}\sigma_I$ reduces ϵ_I'' to three-fourths of its value in simple tension.

Figure 8 shows that the octahedral-shear theory underestimates and the maximum-shear theory overestimates the plastic strain in the region where these strains are of a magnitude comparable with the elastic strains. The prediction of the slip theory is intermediate between those of octahedral shear and maximum shear and is in excellent agreement with the test data for stress ratio 0.5. The data for stress ratio 2, which might be expected to coincide with the data for stress ratio 0.5, cannot be regarded as in good agreement with the slip theory. These data were obtained by applying internal pressure alone to the tube and, on account

of the finite thickness of the wall, actually correspond to a stress ratio of 2.06; however, this does not appear to account for the discrepancy. Calculations based on octahedral-shear theory imply that the plastic strains ϵ_I'' for stress ratios 2 and 2.06 should differ not more than a few percent, and it is therefore felt that the differences between the experimental results for stress ratios 0.5 and 2 noted in figure 8 primarily represent scatter in the material properties. In any event, the test data taken as a whole are in better agreement with the slip theory than with either octahedral-shear theory or maximum-shear theory. According to all three theories of plasticity, the transverse plastic strain ϵ_{II}'' is zero. As indicated in the table below, the plastic strain computed from the data was always less than 0.001:

$\frac{\sigma_I}{\sigma_L}$	ϵ_{II}''	
	$\frac{\sigma_y}{\sigma_x} = 0.5$	$\frac{\sigma_y}{\sigma_x} = 2$
1	0	0
1.2	$-.17 \times 10^{-3}$	$-.01 \times 10^{-3}$
1.4	-.19	-.10
1.6	-.40	-.40
1.8	-.90	-.90

The loading function proposed by Drucker (reference 4) has not been considered in the present comparison because the specification of loading function alone is not enough to determine plastic stress-strain relations.

CONCLUDING REMARKS

The slip theory of plasticity, which is derived from physical considerations with respect to the mechanism of plastic deformation, has previously been checked against experiments involving continuously variable stress ratios. In the present paper the slip theory is shown to be in good agreement with biaxial-tension data involving constant stress ratios. The octahedral-shear and maximum-shear theories are shown to be in poorer agreement with the test data.

Langley Aeronautical Laboratory
National Advisory Committee for Aeronautics
Langley Air Force Base, Va., November 10, 1949

REFERENCES

1. Batdorf, S. B., and Budiansky, Bernard: A Mathematical Theory of Plasticity Based on the Concept of Slip. NACA TN 1871, 1949.

2. Osgood, William R.: Combined-Stress Tests on 24S-T Aluminum Alloy Tubes. Jour. Appl. Mech., vol. 14, no. 2, June 1947, pp. A-147 - A-153.

3. Peters, Roger W., Dow, Norris F., and Batdorf, S. B.: Preliminary Experiments for Testing Basic Assumptions of Plasticity Theories. Proc. Soc. Exp. Stress Analysis, vol. 7, no. 2 (presented at the Spring Meeting, May 1949).

4. Drucker, D. C.: Relation of Experiments to Mathematical Theories of Plasticity. Paper No. 49-APM-5 presented at the National Conference of Appl. Mech. Div., A.S.M.E., Ann Arbor, Mich., June 13-15, 1949.

5. Prager, William: The Stress-Strain Laws of the Mathematical Theory of Plasticity - A Survey of Recent Progress. Jour. Appl. Mech., vol. 15, no. 3, Sept. 1948, pp. 226-233.

BIBLIOGRAPHY

1. Lode, W.: Versuche über den Einfluss der mittleren Hauptspannung auf das Fliessen der Metalle Eisen, Kupfer, und Nickel. Zeitschrift für Physik, Bd 36, Hefte 11 and 12, May 11, 1926, pp. 913–939.

2. Schmidt, R.: Über den Zusammenhang von Spannungen und Formänderungen im Verfestigungsgebiet. Ing.-Archiv, Bd. III, Heft 3, 1932, pp. 215–235.

3. Nadai, A., and Davis, E. A.: Plastic Behavior of Metals in the Strain-Hardening Range. Parts I and II. Jour. Appl. Phys., vol. 8, no. 3, March 1937, pp. 205–217.

4. Davis, E. A.: Combined Tension–Torsion Tests on a 0.35 Per Cent Carbon Steel. Trans. A.S.M.E., vol. 62, no. 7, Oct. 1940, pp. 577–586.

5. Low, John R., Jr., and Prater, T. A.: Plastic Flow of Aluminum Aircraft Sheet under Combined Loads II. (NA–150), OSRD No. 4052, serial no. M–328, War Metallurgy Div., NDRC, Aug. 1944.

6. Dorn, J. E., and Thomsen, E. G.: The Effect of Combined Stresses on the Ductility of Metals. OSRD No. 3218, serial no. M–213, War Metallurgy Div., NDRC, Feb. 2, 1944.

7. Gensamer, M., Landford, W. T., Jr., Prater, T. A., Vajda, John, and Ransom, J. T.: Plastic Flow of Aluminum Aircraft Sheet under Combined Loads (NA–149) (NA–150). II – Forming Limits for Aircraft Sheets at Room Temperature. OSRD No. 5283, serial no. M–528, War Metallurgy Div., NDRC, June 29, 1945.

8. Davis, E. A.: Yielding and Fracture of Medium-Carbon Steel under Combined Stress. Jour. Appl. Mech., vol. 12, no. 1, March 1945, pp. A-13 – A–24.

9. Cunningham, D. M., Thomsen, E. G., and Dorn, J. E.: Plastic Flow of a Magnesium Alloy under Biaxial Stresses. Proc. A.S.T.M., vol. 47, 1947, pp. 546–553.

10. Marin, Joseph, Faupel, J. H., Dutton, V. L., and Brossman, M. W.: Biaxial Plastic Stress–Strain Relations for 24S–T Aluminum Alloy. NACA TN 1536, 1948.

11. Marin, Joseph, Faupel, J. H., and Dutton, V. L.: Tension–Compression Biaxial Plastic Stress–Strain Relations for ALCOA 24S–T. Tech. Rep. No. 5694, Air Materiel Command (Wright–Patterson Air Force Base), April 1948.

12. Thomsen, E. G., Cornet, I., Lotze, I., and Dorn, J. E.: Investigation on the Validity of an Ideal Theory of Elasto-Plasticity for Wrought Aluminum Alloys. NACA TN 1552, 1948.

13. Fraenkel, S. J.: Experimental Studies of Biaxially Stressed Mild Steel in the Plastic Range. Jour. Appl. Mech., vol. 15, no. 3, Sept. 1948, pp. 193-200.

14. Davis, H. E., and Parker, E. R.: Behavior of Steel under Biaxial Stress as Determined by Tests on Tubes. Jour. Appl. Mech., vol. 15, no. 3, Sept. 1948, pp. 201-215.

15. Gleyzal, A.: Plastic Deformation of a Circular Diaphragm under Pressure. Jour. Appl. Mech., vol. 15, no. 3, Sept. 1948, pp. 288-296.

TABLE 1

CALCULATED g–VALUES

$$\left[\epsilon''\left(\frac{\sigma}{\sigma_L}\right) = \sum a_n g_n\left(\frac{\sigma}{\sigma_L}\right)\right]$$

σ/σ_L	g_1	g_2	g_3	g_4	g_5
1.10	0.0311486	0.0020860	0.0001560	0.0000137	---------
1.25	.1671619	.0281396	.0053115	.0010741	0.0002206
1.40	.3744986	.1004147	.0308275	.0099447	.0033785
1.60	.7211448	.2948256	.1354768	.0651761	.0336644
1.80	1.1965026	.6448685	.3883228	.2487629	.1656213

NACA

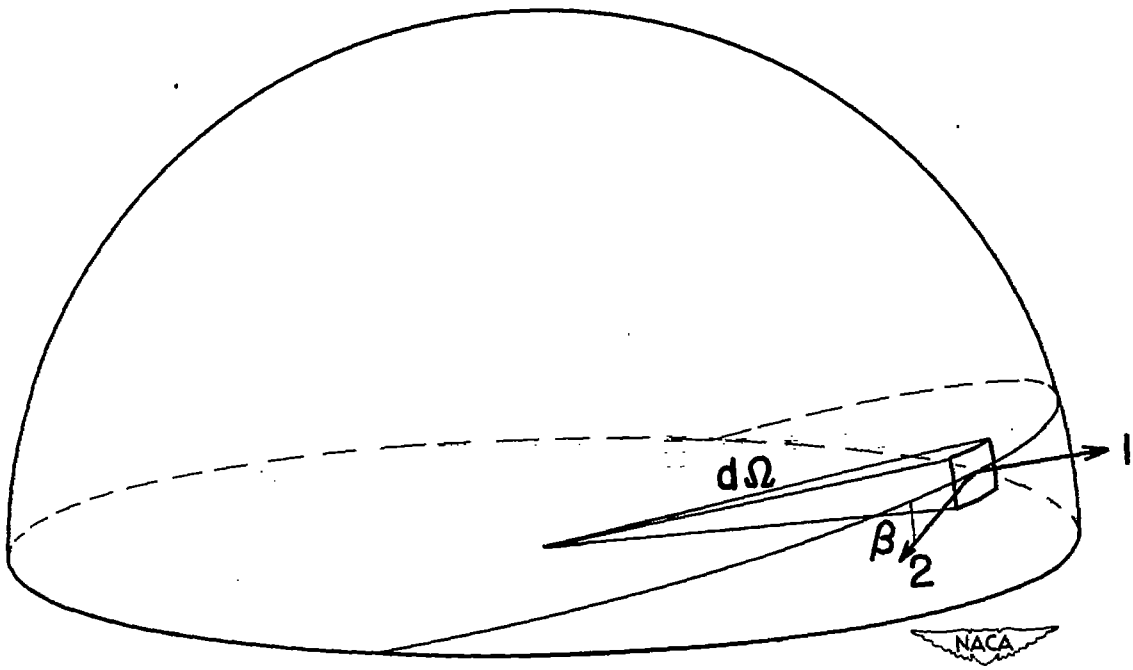

Figure l.- Slip-plane normal, l, and direction of slip, 2, for typical slip plane.

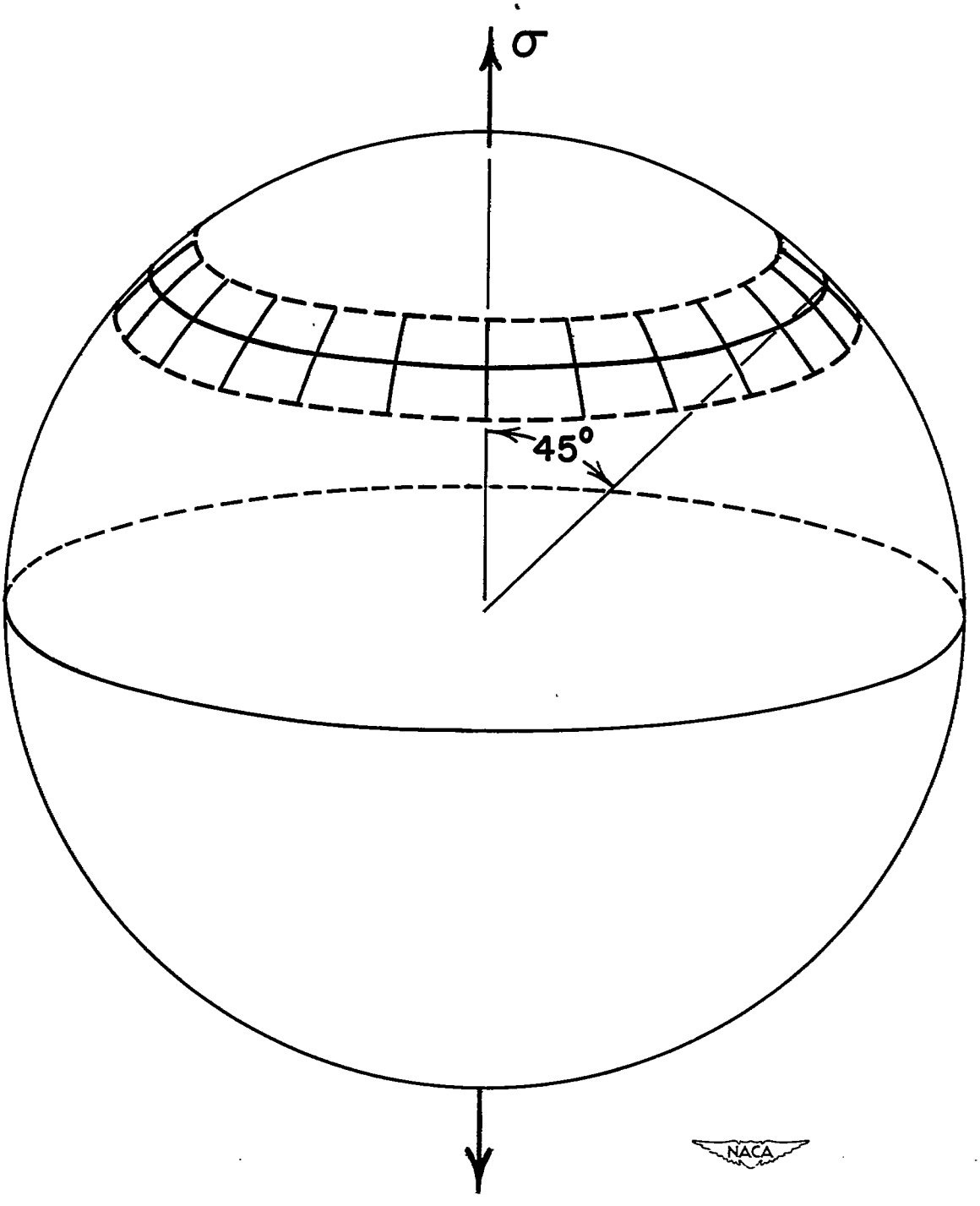

Figure 2.- Zone of intersections of slip-plane normals with unit sphere for simple tension.

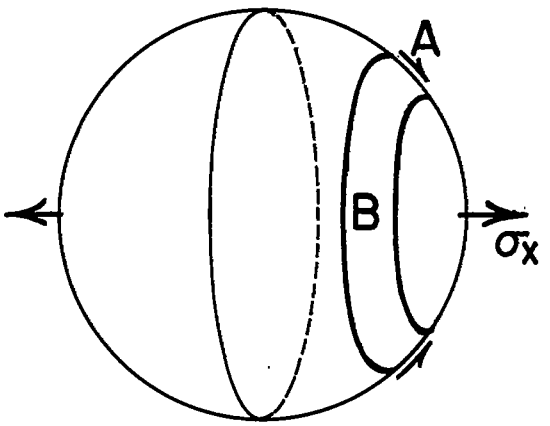

(a) Tension in x direction.

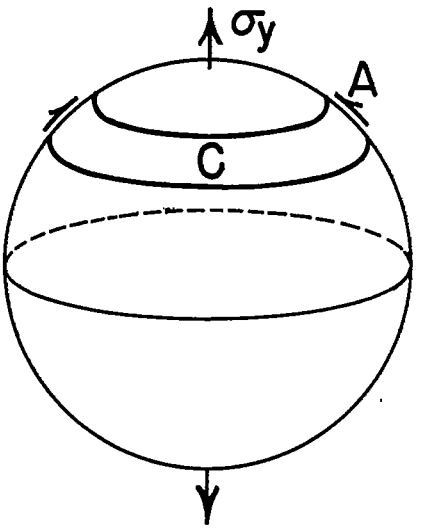

(b) Tension in y direction.

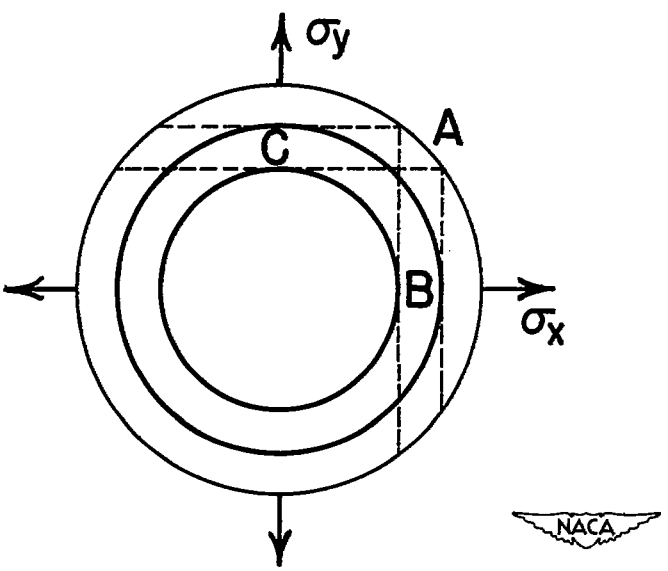

(c) Combined tension, $\sigma_x = \sigma_y$.

Figure 3. - Zones of intersections of slip-plane normals with unit sphere.

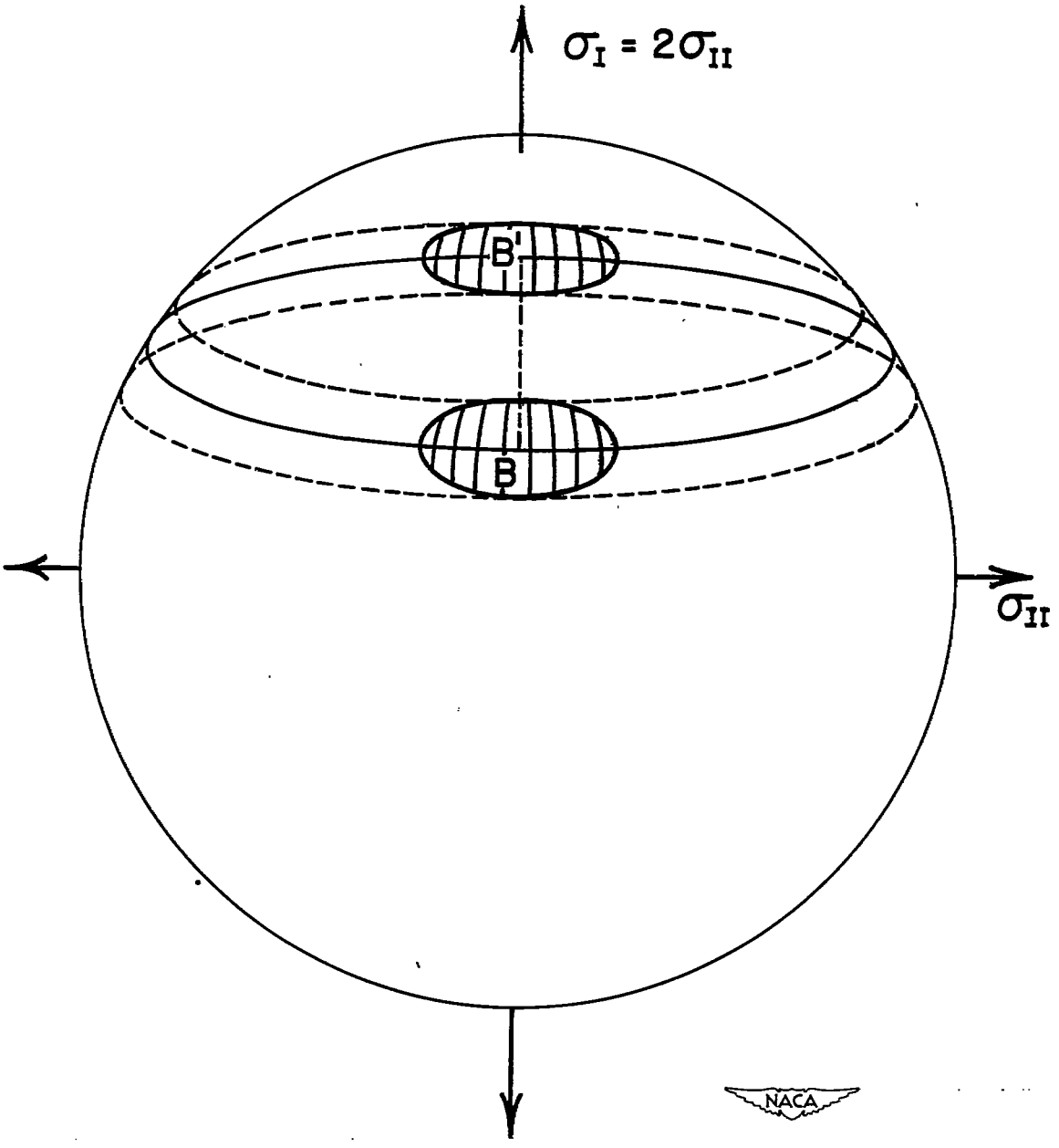

Figure 4.- Zones of intersections of slip-plane normals with unit sphere when $\sigma_I = 2\sigma_{II}$, $\sigma_{III}=0$.

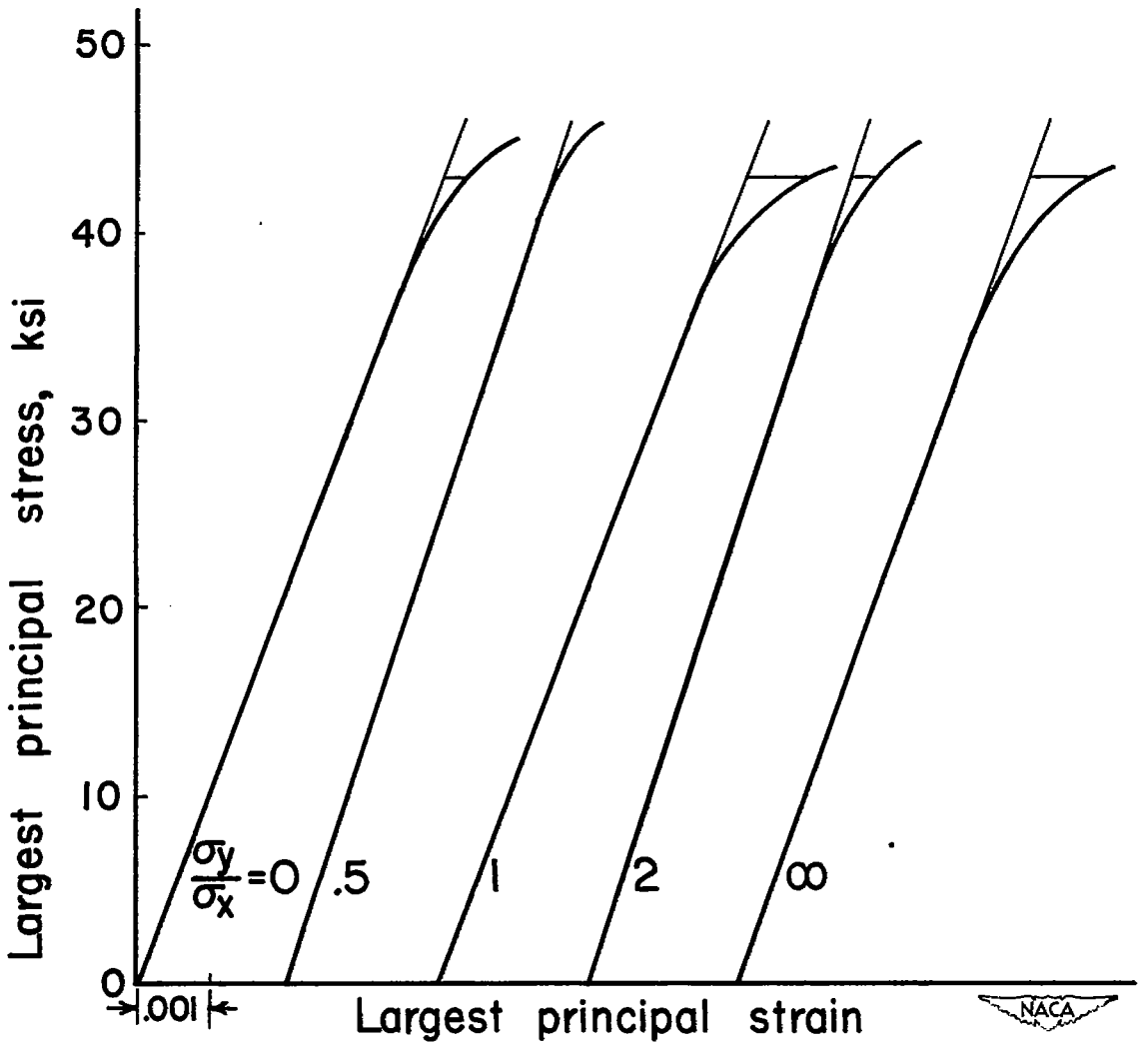

Figure 5. - Experimental curve of largest principal stress against largest principal strain for various stress ratios. (Curve for stress ratio = 1 is compressive stress-strain curve in radial direction.)

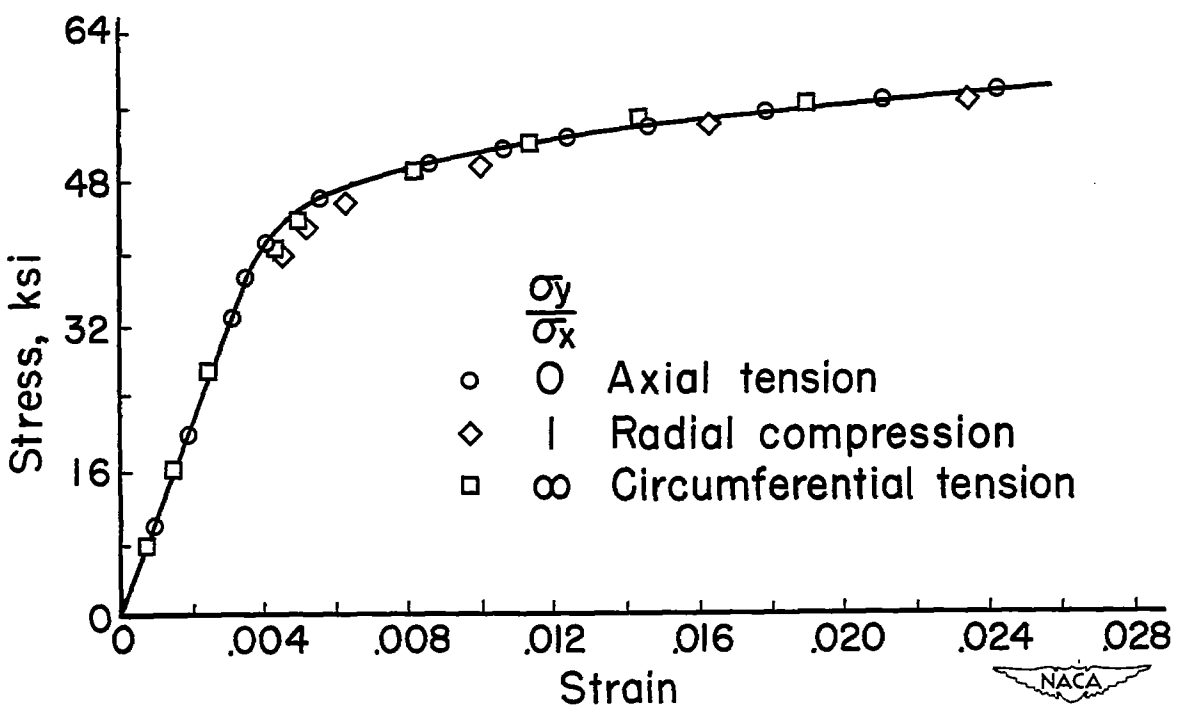

Figure 6.- Stress-strain relations in principal directions. (Curve plotted for axial tension only.)

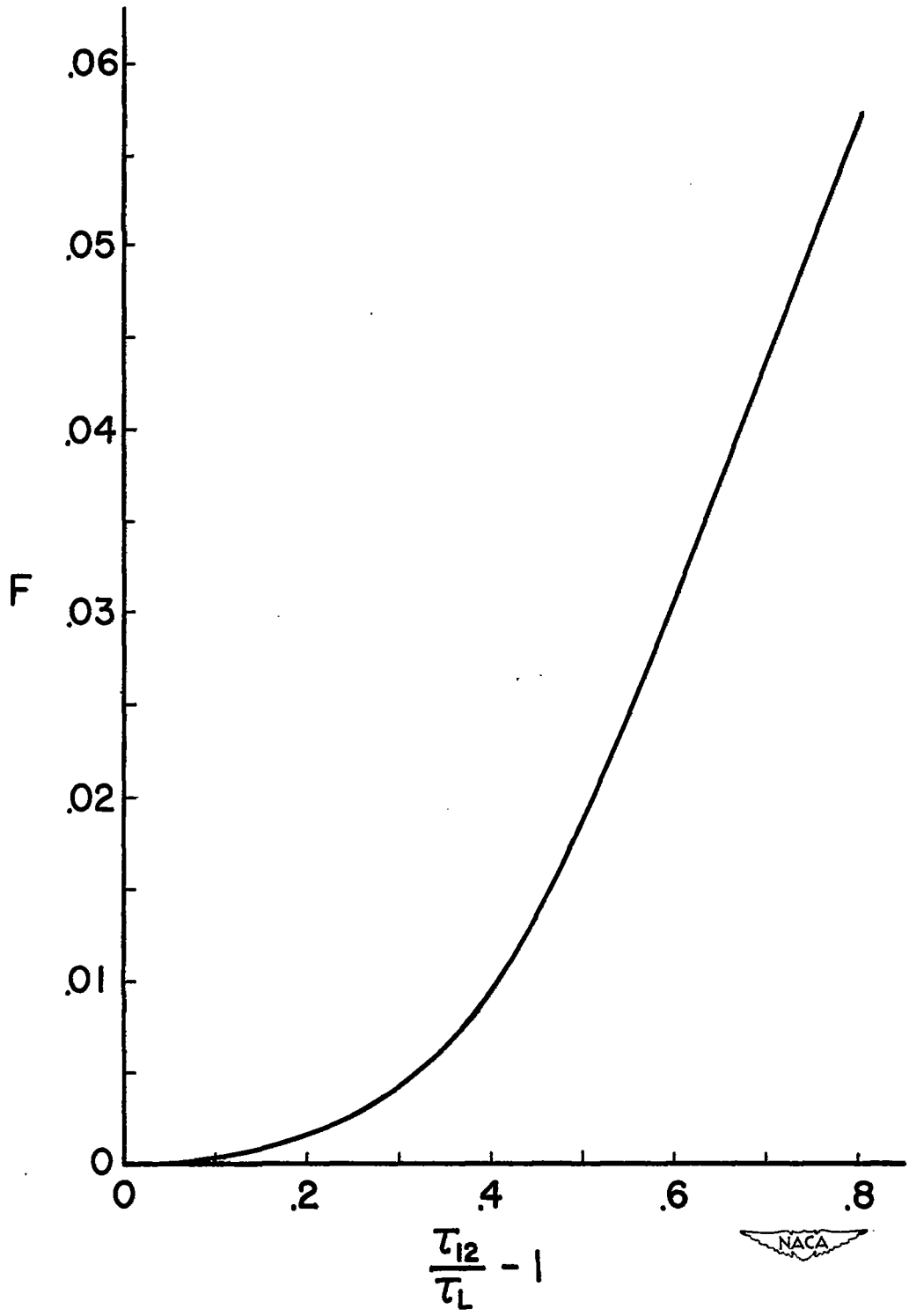

Figure 7. - Plot of characteristic shear function of material.

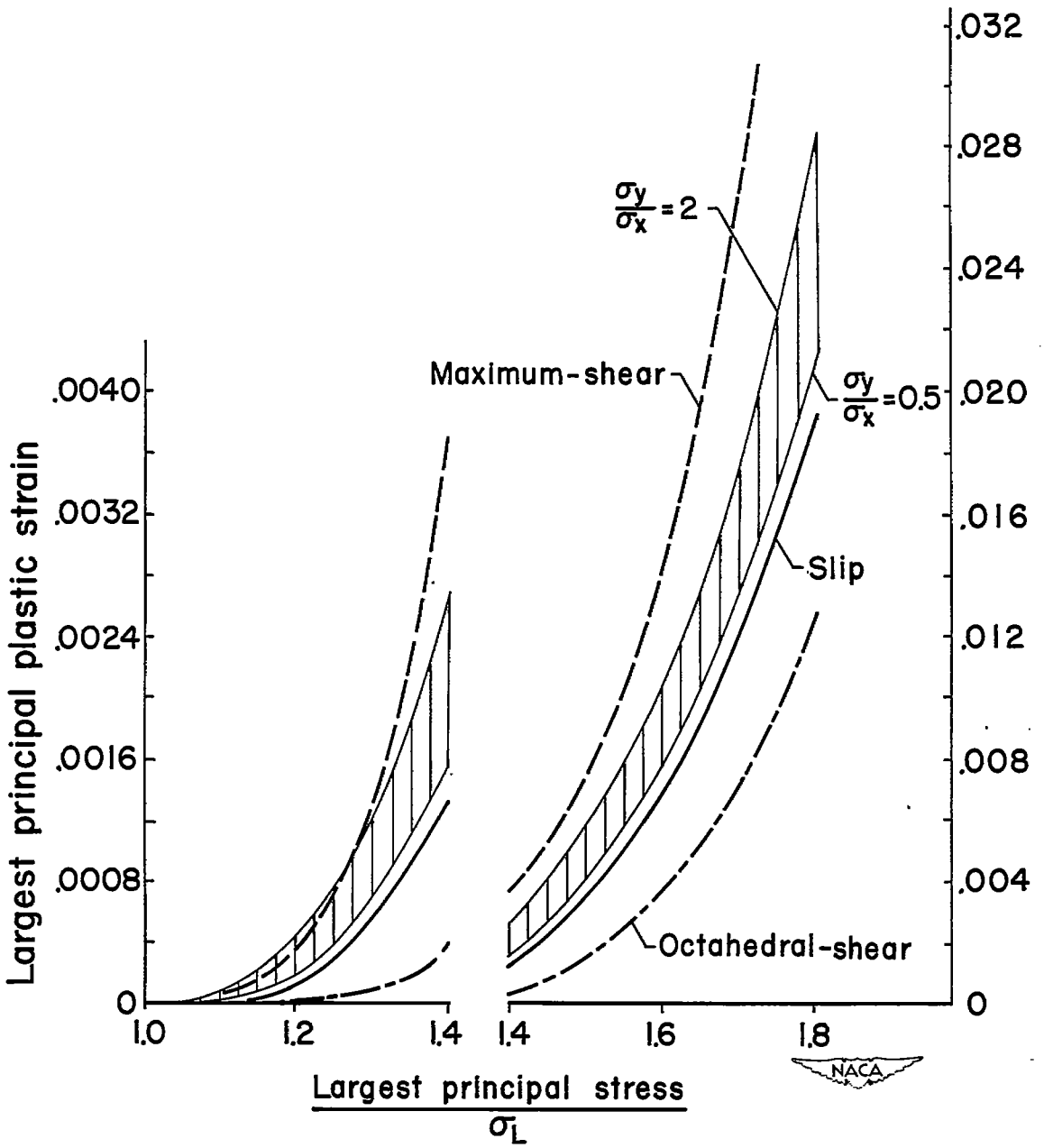

Figure 8.- Comparison of plastic-strain theories with experimental data.